Simulations of LGM climate of East Asia by regional climate model

ZHENG Yiqun (郑益群)[1,2], YU Ge (于 革)[1], WANG Sumin (王苏民)[1], XUE Bin (薛 滨)[1], LIU Huaqiang (刘华强)[2] & ZENG Xinmin (曾新民)[2]

1. Nanjing Institute of Geography and Limnology, Chinese Academy of Sciences, Nanjing 210008, China;
2. Institute of Meteorology, PLA University of Science and Technology , Nanjing 211101, China
Correspondence should be addressed to Zheng Yiqun (email: yqzheng@niglas.ac.cn)

Received August 21, 2002

Abstract Climate conditions in the Last Glacial Maximum (LGM) were remarkably different from the present ones. Adopting a regional climate model (RCM) which has included a detailed land surface scheme, LGM climate of East Asia has been simulated. The effects of vegetation changes on LGM climate have been diagnosed by adding forces of LGM paleovegetation reconstructed from the geological records. The results of the simulations by RCM indicate that large decreases in whole year temperature of East Asia continent caused strongly enhanced winter monsoon and weakened summer monsoon. The strengthening and westward-stretching of the Subtropical High of West-Pacific are the key reasons of decreases of LGM summer precipitation in eastern China. Precipitation and effective precipitation were increased in the Tibetan Plateau and Middle-Asia, while the humid condition in the Tibetan Plateau was mainly caused by increase of precipitation. Accumulated snow of LGM was also increased in the Tibetan Plateau, which was helpful to developing glacier and permafrost. This experiment has simulated that the frozen soil areas extend southward to 30° N. In LGM climate simulation, climate effects caused by external forces were amplified by added paleovegetation, therefore, decreases of temperature, changes of precipitation and snowfall, and other climatic parameters were further strengthened, making the simulation results more approach to geological evidences.

Keywords: LGM, regional climate modelling, vegetation changes, East Asian monsoon.

DOI: 10.1360/03yd0502

Climate conditions in the Last Glacial Maximum (LGM) were remarkably different from the present ones. LGM global mean temperature was 5℃－10℃ drop but precipitation decreases commonly. LGM has become the key phase to reconstruct the earth environmental field, retrieve extreme cold climate conditions, and test the earth orbit forecasting, and underlying surface feedback[1]. LGM climate and the environments are important subjects of the study of global change.

“Paleoclimate Modeling Intercomparison Project” (PMIP) designed paleoclimate modeling experiments to simulate LGM climate, using Global Circulation Model (GCM) under the LGM boundary conditions of solar radiation, icesheets, CO_2 concentration, sea surface temperature (SST) and sea ice, etc. Most simulations of the GCM can be compared with geological data in lots of regions (Africa, North America and Europe), but only a few results can catch the climate characters of East Asia well[2]. It is possible that monsoon system in the East Asia is more complex than that of South Asia and Africa, and difficult to probe the moisture sources of the increased precipitation in the Tibetan Plateau.

Recent studies on the effects of vegetation changes on paleoclimate show that the feedbacks between atmosphere and vegetation enlarge the climate variation driven by the earth orbit forcing, and improve the simulation results[3—6]. Most GCM simulations of LGM climate, due to their low resolutions, could not fully satisfy the requirement of study for vegetation feedbacks on regional climate, and have limitations for East Asian regional climate study. Regional Climate Model (RCM) can more efficiently simulate the interactions of various scales of inner and external forces, which can catch the changes in the regional climate preferably and get high-resolution climatic images. However, the RCM is more sensitive in experiments by the external forcing, making this become a tough topic to work on. We only read in efforts a few literatures (Hostetler et al.[7]).

The present work simulated East Asian climate at the LGM by using the Regional Climate Model (RegCM2) including a detailed land surface scheme, and tested the effects of vegetation on East Asian monsoon by using PMIP (1995) standard forces (solar radiation, ice sheets, CO_2 content and sea surface temperature) and reasonable LGM paleovegetations[8].

1 Model and experimental scheme

Model adopted in this study is Regional Climate Model version 2 (RegCM2) of the National Center for Atmospheric Research (NCAR, USA) developed by Giorgi et al.[9]. BATS1e scheme adopted in this model describing land surface process was designed by Dickinson. This scheme can calculate exchange of water/thermal flux between soil/vegetation and atmosphere in detail. The physical process in boundary layer can be described more realistically and the effect of simulation can be improved after we employ turbulence kinetic energy (TKE) closure scheme in RegCM2[10]. In addition, we modified the calculation of sun-earth distance parameter (set as constant in original model) for the present paleoclimate simulation. The experimental domain covers East Asia including the Qinghai-Tibetan Plateau. The model has horizontal grid points of 72×50, grid length of 120 km, and 11 levels in vertical profile. The main features of LGM external forces have been included in this domain, i.e. Quaternary icesheets in the Northern Hemisphere, lower SST, reduced sea area and enlarged land area, degraded vegetation, etc. In this work we employed the simulation results of NCAR CCM1[11] of both 0ka B.P. and LGM simulation as initial and lateral boundary fields, and adopted sponge lateral boundary of five-grid-point-wide-buffer zone. We took 6 years to do all the experiments and used the average in the last 5 years for climatological analyses.

To gain insight into the LGM climatic responses to changed vegetation, we designed 3 experiments: 0k B.P. control run (E0ka), LGM PMIP experiment (E21kaP) and LGM experiment (E21kaF). We used 0ka B.P. control run to test the simulate ability of model, which can be regarded as base points of LGM climatic changes. Table 1 lists the main features of the boundary conditions and parameter setting for the present experiments.

Table 1 Earth orbital parameter and boundary conditions

Setting	Earth orbit parameter[12]			CO_2 content	SST	Icesheet and land surface
	eccentricity	perihelion	obliquity			
E0ka	0.016724	282.04	23.446	345 mg •kg^{-1}	modern	modern vegetation
E21kaP	0.018994	294.42	22.949	200 mg •kg^{-1}	CLIMAP-based LGM SST	Quaternary icesheet and modern vegetation
E21kaF	0.018994	294.42	22.949	200 mg •kg^{-1}	CLIMAP-based LGM SST	Quaternary icesheet and 21 ka vegetation

Previous studies[13—15] have suggested that LGM SST drop estimated by the CLIMAP program was smaller than that of the geological records and there were not warmer tropical seas during the LGM[16]. Due to lack of updated SST data, we still use February and August SST of the CLIMAP data and a method of sine type interpolation to obtain the SST of each month. We modified partial grids of SST according to geological records, and interpolated point-data of modern vegetation and paleovegetation into grid-data in the same scale of the RCM model. Fig. 1(a) and (b) depicts the land surface distributions of E0ka and E21kaF respectively. Major changes in E21kaP are that the icesheet area in high latitudes and land-sea distributions is much different from that at the E0ka.

Fig. 1 shows the significant difference of land surface condition between LGM and 0ka B.P. Because a large amount of sea water had been transferred into ice and stored in land icesheets, there were about 6.3×10^5 km^2 continental shelves which were exposed and became land in the Yellow Sea[17]. The exposed sea bottoms were desert coverage at the LGM according to resumed type by BIOME 6000[18]. In experimental domains, there were about 36% changes of land vegetation coverage between LGM and 0ka B.P., which mainly included increased large area of tundra distributed at northern 60° N in the modern time and was replaced by ice sheets during the LGM and decreased large area of Taiga replaced by tundra, and decreased area of subtropical forest vegetation in East Asia because the forests moved southward and shrank to south of the Tropic of Cancer[8].

2 Results of the simulations

Fig. 2(a) depicts the temporal variations of land surface temperature (whole area average), total soil (about 3m depth), water content (whole area average), 500hPa geopotential height (Yangtze-Huai valleys average) and precipitation average of Yangtze-Huai valleys in the control run, showing that the simulated temperature is of an evident seasonal feature, with a shorter spinup time, namely, each year has resemble amplitude of temperature variation. The root zone soil moisture needs longer spinup time. After one year each layer of soils can be adjusted to an equilibrium condition, suggesting that if eliminating first year’s integral data, the normals of simulation can be treated as climatic equilibrium status.

The precipitation in Yangtze-Huai valleys also presented an evidence of seasonal variation, in which there were two precipitation peaks in May and September. When the areas were controlled

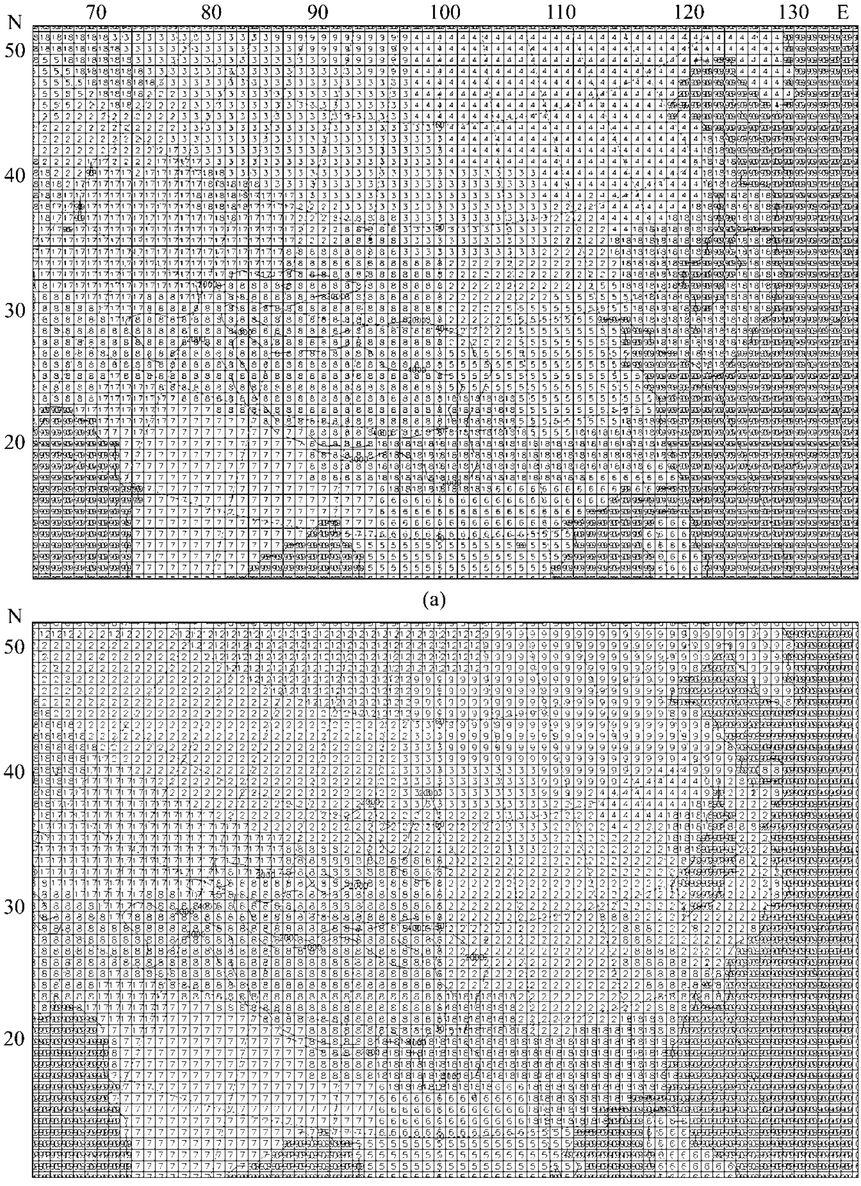

Fig. 1. The land surface distribution of 0ka B.P.(a) and LGM (b). 99, Water; 1, crop; 2, short grass; 3, evergreen needle leaf tree; 4, deciduous needle leaf tree; 5, deciduous broadleaf tree; 6, evergreen broadleaf tree; 7, tall grass; 8, desert; 9, tundra; 10, irrigation crop; 11, semi-desert; 12, ice; 13, bog or marsh; 14, inland water; 15, sea; 16, evergreen shrub; 17, deciduous shrub; 18, mixed tree.

by Subtropical High in July—August, a precipitation abruptly decreased and condition was drying in the season. This phenomenon can be explained by the concerned climate rules. Fig. 2(b) plots a time series of 5-years mean of land surface air temperature of Nanjing (upper), Balkhash (middle), and Hami (lower), showing that the errors between simulation and observation are less than 3℃

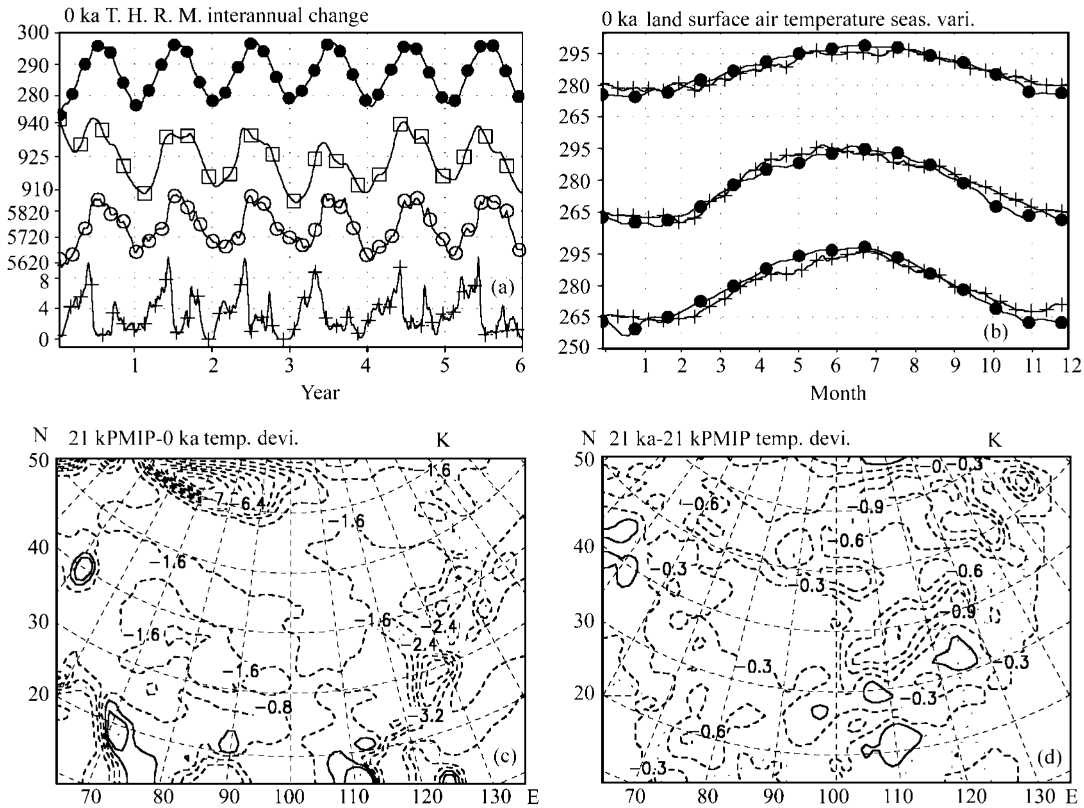

Fig. 2. The changes of land surface temperature, precipitation, soil humidity and geopotential height of 500 hPa. (a) The interannual changes of land surface temperature (●, whole region mean), soil water content (□, whole region mean), geopotential height of 500hPa (○, Yantze-Huai valley) and precipitation (+, Yantze-Huai valley)in 0ka control run; (b) the land surface air temperature seasonal changes of Nanjing (upper), Balkhash(middle) and Hami(lower) in 0ka control run. The crosses lines are simulation and the filled circles are observation; (c) E21kaP-E0ka annual mean land surface temperature differences; (d) E21kaF-E21kaP annual mean land surface temperature differences. Temperature, ℃; geopotential height, m; precipitation, mm/d; soil water content, mm.

in most seasons. Lots of previous sensitivity experiments have indicated that this kind of deviation is a systematic error but does not seriously affect the relative comparison between the LGM and present simulations. Based on outputs of the 0ka B.P. control run, the RegCM2 has higher ability to imitate seasonal evolution of precipitation and the forming and advancing of East Asian summer monsoon. The accumulating and melting snow covers are reasonable, and could produce reasonable climatic response forced by land surface changes (e.g. snow cover, soil temperature and humidity, vegetation)[19]. Thus the RegCM2 is able to reproduce the regional climate.

2.1 Land surface temperature and air temperature

The key feature of LGM is global cooling. From the annual mean of land surface temperature difference of E21kap-E0ka (fig. 2(c)), we can see the temperature drops in most experiment regions, especially in higher-latitudes where Quaternary icesheets were located, with more than 9℃

decrease; but in mid-low latitudes regions, the annual mean is only about 2℃. Geological data[14,16,20] reveal that the LGM temperature decreases varied zonally, exceeding 15℃ in high-latitude zone, 4℃—12℃ in middle-latitudes in China, and 2℃—4℃ in low-latitudes. The RegCM2 simulated a weaker temperature decrease compared with that of geological data. This result maybe relates to the following reasons. Firstly, the effects of LGM icesheets on temperature decrease have not yet been completely expressed in our regional window. The effects of icesheets on temperature mainly depend on its extent, and cause a temperature decrease at down-wind region through atmospheric transferring[21]. Secondly, higher CLIMAP-based SST adopted in this study would lead to a small amount of temperature decrease due to the forces by ocean, and hinder the effect of advection cooling due to effects of icesheet zone in the high latitudes into the mid-low latitudes. Webb et al.[22] pointed out that employing CLIMAP-based SST would bring a larger ocean heat transfer (OHT) and a larger ocean heat convergence (OHC), and limit the extend of icesheets cooling. From E21kaF experiment, we find that the simulation produced much cooling in most regions after the LGM vegetation was introduced. The decreased temperature at cooling center reaches up to about 1℃ (fig. 2(d)), improving the simulation result of land temperature to some extent.

From the comparisons of seasonal temperature variations in all experiments (figure not shown), we find that LGM cooling of summer is more notable than that of winter, except eastern China and Yellow sea. Kutzbach et al. [11] showed that based on their LGM simulation, summer cooling is obvious than that of winter in icesheets areas, thus making a smaller annual temperature variation. In addition, simulated LGM temperature decrease can extend to high levels (higher than 100hPa), showing that LGM temperature decrease is a profound atmospheric phenomenon. Their results are consistent with our simulation output.

2.2 Precipitation (P) and effective precipitation (P-E)

Comparison of annual mean precipitation rate in E0ka (figure omitted) with that in E21kaF (fig. 3(a)) indicates that precipitation in East Asian was evidently decreased during the LGM. Main precipitation belt withdrew southward by nearly 10 latitudes, and center intensity of precipitation weakened by about 1mm/d (nearly 30% lower than 0 ka). In western China, especially on south side of the Tibetan Plateau, the simulated amplitude of precipitation agrees with the reconstructed precipitation (filled dots in fig. 3(a)) by using water-thermal balance model based on geological data[23]. The East-Asian climate records from lakes, glaciers and loess also show that the low-level lakes or dry basins in eastern China and 23° N south of south Asia reflect a very dry climate at LGM[24]. However, in western China, there were high-level and fresh water lakes during 21—17 ka B.P.[25,26]. Glaciers on the Tibetan mountains were largely advantaged, which increased 7.5 times compared with those at present[27]. In addition, pollen data-based reconstruction at LGM showed an extending of wetlands in Tibetan Plateau and North and Northeast China[28], reflecting

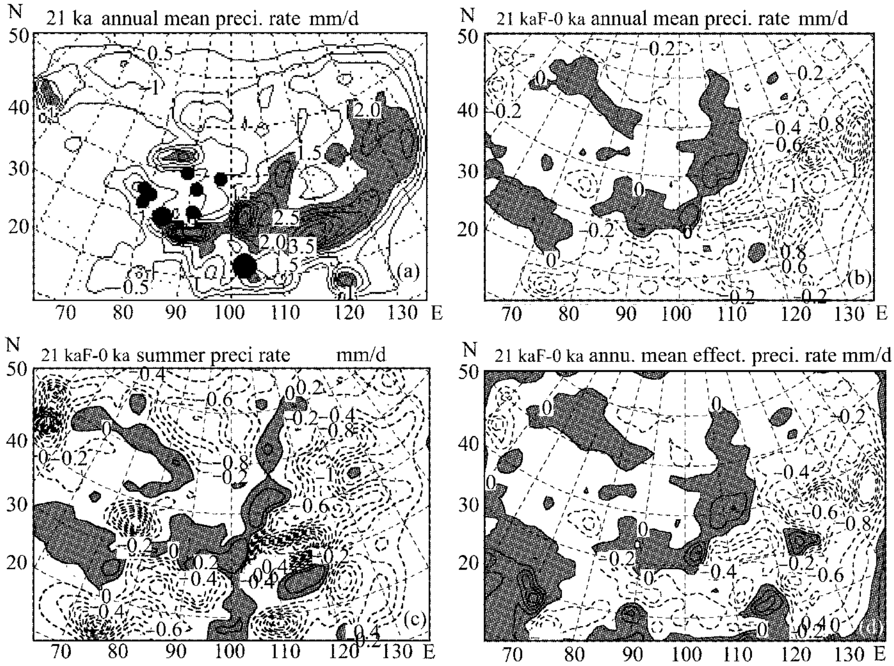

Fig. 3. Simulated annual mean precipitation rate, effective precipitation and resumed precipitation by water-thermal balance model[23]. (a) E21kaF precipitation, filled circles are resumed precipitation; (b) E21kaF-E0ka annual precipitation differences; (c) E21kaF-E0ka summer precipitation differences; (d) E21kaF-E0ka effective precipitation differences. ●, 2—3; ●, 1.5—2; ●, 1—1.5; ●, 0.5—1; ●, 0—0.5 (mm/d).

a wet and cold climate. From the distribution of E21kaF-E0ka annual mean precipitation (fig. 3(b)), we can see that precipitation was remarkably decreased in eastern China and the mid-south India, but increased in west of Sichuan Province and the Tibetan Plateau. Lake level studies[25] indicated that the wet-condition pattern in western China constituted a consistent wet belt from the Mediterranean region, central Asia to western China at 90—95°E. The conditions can be explained by the dominance of glacial anticyclone in northern Europe and the mid-high latitude continental cooling of the large permafrost areas in Mongolian-Siberian plateaus during the LGM. They could force a southward shift of the Westerly and create different atmospheric circulations. However, in contrast with wet conditions, much drier conditions than today occurred in eastern China and mid-south India. Both high and low lake levels occurred in Xinjiang, suggesting that this region was a transitional belt between northern Eurasian arid conditions and Tibetan humid conditions. Our simulated increase of precipitation in Yellow River valleys (Inner Mongolia) is not consistent with relative geological data, expecting for improving simulations and validating by more geological evidence. From the analysis of seasonal variations of simulated LGM precipitation, the precipitation changes in winter are smaller than those in summer (fig. 3(c)), suggesting that a summer-precipitation pattern dominated the framework of precipitation during the LGM. In addition, the simulations show quite similar feature of LGM annual pattern to the summer precipitation. The low summer and annual precipitations were caused by the weakening of LGM summer monsoon. The distribution of effective precipitation (P-E, fig. 3(d)) is consistent with patterns of precipitation (fig. 3(b)). Because of the increases of precipitation and the P-E in the Tibetan Plateau, the changes of precipitation are one of the important factors making high-level lakes emerge at LGM over the areas.

Comparing simulated LGM precipitation in this work with previous output by GCM [2,11,29], we can see that although all of the models could simulate a dry climate condition in East Asia and wet climate condition in West Asia, the center of precipitation has been simulated in different places. The distribution of precipitation center simulated by RegCM2 is closer to that of simulations by GCM, but we can obtain more detailed precipitation image owing to improvement of resolution in regional climate model that the locations are consistent with related geological evidence. The simulated precipitation is further consistent with geological data after adopting LGM vegetation. Net decreases of precipitation caused directly by vegetation effects are 1 mm/d in annual mean and 1.6 mm/d in summer months.

2.3 Atmospheric humidity and circulation

Simulated atmospheric humidity was obviously decreased at LGM in most areas, especially in the simulation adopting paleovegetation. The decreased value at 850 hPa reaches up to 1.2 g/kg in the center (fig. 4(a)), indicating that LGM was a drier and colder climate period than today. The humidity was less changed in Tibetan Plateau and Central Asia. Indeed there were somewhat increases, especially in summer. Comparing humidity with precipitation, we can find that there is a good correlation between humidity decrease and precipitation decrease, implying that decrease of LGM humidity is the most important reason for the precipitation decrease in this period. Vegetation degeneration produced an intensified effect on humidity decrease, the decrease of which directly caused by vegetation change can exceed 1 g/kg.

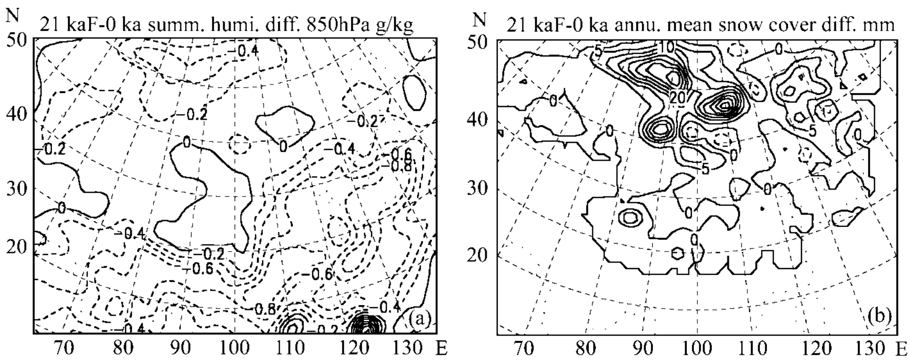

Fig. 4. E21kaF-E0ka specific humidity and snow cover differences. (a) Summer specific humidity at 850 hPa, unit: g/kg; (b) annual mean snow cover, unit: water equivalent.

Along with the changes of water-energy transferring in air-earth system, the circulation got an obvious adjustment, and formed a new pattern of circulation different from 0ka B.P. From the analyses of winter 500hPa deviation circulation, we can find that there were obvious strengthening of anticyclonic circulation at down-wind of the icesheets, leading to the north flow intensified in eastern China that caused a stronger East Asian winter monsoon in LGM. The records of sediments in East China Sea show that more materials are supplied by land source during LGM, indicating an intensified winter monsoon[30]. The summer north flow was intensified in eastern China, implying the reduction of East Asian summer monsoon. Especially in E21kaF including degeneration vegetation coverage, the northern boundary of southerly wind retreated by nearly 8° latitudes, e.g. southward to about 40°N. The comparison of changes of precipitation with circulation between LGM and 0ka B.P. indicates that the decrease of summer precipitation in eastern China is related to the westward stretching of Pacific Subtropical High and its enhancement over this region.

2.4 Snow cover and soil moisture

Due to the decreases of precipitation and temperature at LGM, there are obvious differences in snow cover, glaciers, permafrost and soil humidity between LGM and 0ka B.P. Kuhle et al.[31] speculated about 1000—1200 m decline of the altitude of glacier equilibrium line (ELA) at LGM. The present simulation shows that snow cover increased in mid-high regions at LGM (fig. 4(b)), especially in high-latitude icesheets areas and the icesheet down-wind areas. The increased snows at the center could exceed 30 mm water equivalent, which was mainly caused by temperature decreases. In addition, remarkable increase of snow cover occurred in Tibetan Plateau, revealing a variation of larger increase on outer side and smaller increase on inner side. These results are consistent with the reviews by Shi Yafeng who cognized that the ELA at 0ka B.P. and LGM present a circular patterns; the decrease of ELA could reach 1000—1200 m at the edge of east-south-west sides of the Tibetan Plateau, but only 300m at the center. The increase of snow cover in the Tibetan Plateau was mainly caused by increased precipitation and decreased temperature. There was perennial snow cover in plateau in favor of the development of glacier, which led to the permafrost extend southward to 30°N at the LGM. Simulated soil water content decreased in most of regions, especially in eastern China. Compared to the precipitation variations, there exists a close correlation between soil humidity and precipitation.

3 Discussion

Analysis of the heat equilibrium condition of land surface indicates that the changes of land absorbing solar radiation are most notable and have more important effect on temperature variation compared to other heat counterbalance. During the LGM the latent heat flux of the land surface was decreased in East Asia, which conducted a decline of atmospheric humidity. However changes of latent heat flux in plateau and Central Asia are less. This result can prove that the increase of effective precipitation in plateau mostly lies on precipitation. Analysis of difference in moisture flux at 850 hPa (figure omitted) shows that the increase of precipitation in plateau was mostly due to the increase of the moisture transportation from outside of Tibet. From the deviation of moisture flux (figure omitted), the moisture transferred from eastern China and northern Bengal Bay to the Tibetan Plateau was stronger than today. This phenomenon indicates that under the climate background of global drying at LGM, some regions could present different moisture changes from others due to adjustment of the vapor transferring that can cause the precipitation increases in these areas.

Precipitation is one of the most important factors in East Asian monsoon region, which can reflect the synthesis feature of circulation and atmospheric thermal and humidity conditions. From the above analysis, we recognize that the atmospheric moisture is an important source to conduct the precipitation changes at the LGM. Due to the declines in SST, soil water content and surface temperature at the LGM, a decrease of surface evapotranspiration in both oceans and continents would occur. This conducted a weaker land-sea water cycle and decreased precipitation. Under a drying climate of the LGM, some regions could become relatively wet owing to additional moisture importing and precipitation increased in these areas, such as the Tibetan Plateau and Central Asia regions.

4 Conclusions

The monsoon climate of East Asia at 0ka B.P. and LGM has been simulated in this paper and the effects of vegetation on LGM climate have been discussed. We simulated the main climatic features of cooling and weaker land-sea water cycle, decreased precipitation, drier conditions, increased continentality, weaker summer monsoon and intensified winter monsoon, when we adopted the forces of high-latitude icesheets, lower SST and CO_2 content in LGM than modern time. Besides these boundary conditions, we employed paleovegetation coverage and obtained the variations of temperature and precipitation of the LGM simulations. This paleovegetation has enlarged the effects of external forcing, and made the simulated result further consistent with geological data. The major conclusions are summarized as below:

(1) Drops in land surface temperature of East Asia at LGM are important factors to enhance the East Asian winter monsoon and to weaken summer monsoon. Paleovegetation would heighten the effects of thermal conditions on the land in LGM simulations, intensify the decrease of temperature, and change in East Asian monsoon.

(2) The simulated precipitation remarkably decreases at LGM compared to 0ka B.P., especially in Japan, eastern China and south India. The westward stretching and enhancement of summer Subtropical High at LGM are the most important reasons to decrease summer precipitation in eastern China. The precipitation and effective precipitation all increase in the Tibetan Plateau and Central Asia at LGM. The effective precipitation increasing in the Tibetan Plateau is mainly caused by increases of precipitation. The simulated precipitation would be more coincident

with the geological data after adopting paleovegetation in the LGM simulation.

(3) The simulated atmospheric humidity decreased at LGM in most regions, indicating that LGM was a drier and colder climate period. Compared to drying in most areas, different moisture changes were simulated in the Tibetan Plateau and Central Asia due to increases in vapor input in these areas.

(4) Increases of snow coverage were modeled in mid-high latitudes at LGM. Snows in the Tibetan Plateau also increased, with more on outer side, less on inner side. This is extremely helpful to depositing perennial snow in the plateau, and is favorable for the development of glacier and permafrost, extending southward to 30° N.

This work preliminarily attempts to use a regional climate model in paleoclimate simulation. Compared with previous simulations conducted by GCM, the RCM's can provide much more details of climate changes and help to comprehend the processes and mechanism of changes of East Asian monsoon. We will make experiments of coupling model of vegetation-hydrology-atmosphere in near future in order to understand climate changes well in East Asian monsoon regions.

Acknowledgements The authors are very grateful to Prof. J. Kutzbach, Dr. P. Behling and Dr. S. Rauscher for providing NCAR CCM1 results of 0 ka B.P./6 ka B.P./21ka B.P. This work is supported jointly by the Innovation Project of Nanjing Institute of Geography and Limnology (Grant No. CXNIGLAS-A02-06), the Innovation Project of the Chinese Academy of Sciences (Grant No. KZCX2-SW-118; KZCX2-108), and the National Natural Science Foundation of China (Grant No. 40102015).

References

1. Pinot, S., Ramstein, G., Harrison, S. P. et al., Tropical paleoclimates at the Last Glacial Maximum:comparison of Paleoclimate Modeling Intercomparison Project (PMIP) simulations and paleodata, Climate Dynamics, 1999, 15: 857—874.
2. Yu, G., Chen, X., Liu, J. et al., Preliminary study on LGM climate simulation and the diagnosis for East Asia, Chinese Sci. Bull., 2001, 46: 364—368.
3. Crowley, T. J., Steven, K. B., Effect of vegetation on an ice-age climate model simulation, J. Geophy. Res., 1997, 102: 16463—16480.
4. Texier, D., Noblet, N. D.., Harrison, S. P. et al., Quantifying the role of biosphere-atmosphere feedbacks in climate change: Coupled model simulations for 6000 years BP and comparison with palaeodata for northern Eurasia and northern Africa, Climate Dynamics, 1997, 13: 865—882.
5. Kubatzki, C., Claussen, M., Simulation of the global bio-geophysical interactions during the Last Glacial Maximum, Climate Dynamics, 1998, 14: 461—471.
6. Wang, H. J., Role of vegetation and soil in the Holocene megathermal climate over China, J. Geophys. Res., 1999, 104: 9361—9367.
7. Hostetler, S. W., Giorgi, F., Bates, G. T. et al., Lake-Atmosphere feedbacks associated with Paleolakes Bonneville and Lahontan, Science, 1994, 263: 665—668.
8. Yu, G., Chen, X., Ni, J. et al., Palaeovegetation of China: A pollen date-based synthesis for the mid-Holocene and Last Glacial Maximum, Journal of Biogeography, 2000, 27: 635—664.
9. Giorgi, F., Marinucci, M. R., Bates, G. T., Development of a Second-Generation Regional Climate Model (RegCM2), Part I: Boundary-Layer and Radiative Transfer Processes, Mon. Wea. Rev., 1993, 121: 2794—2813.
10. Zheng, Y. Q., Miao, M. Q., Qian, Y. F., Turbulence kinetic energy closure scheme applied into regional climate modeling, Acta Meteorologica Sinica (in Chinese), 1999. 57(6): 641—650.
11. Kutzbach, J., Gallimore, G, Harrison, S. et al., Climate and BIOME simulations for the past 21 000 years, Quaternary Science Reviews, 1998, 17: 473—506.

12. Berger, A. L., Long-term variations of daily insolation and Quaternary climatic changes, J Atmos Sci, 1978, 35: 2362—2367.
13. Guilderson, T. P., Fairbanks, R. G., Rubenstone, J. L., Tropical temperature variations since 20 000 years ago: Modulating interhemispheric climate change, Science, 1994, 263: 663—665.
14. Anderson, D. M., Webb, R. S., Ice-age tropics revised, Nature, 1994, 364: 23—24.
15. Yao, T. D., The abrupt climatic changes on the Tibetan Plateau during the last ice age, Science in China, Ser. D, 1999, 42(4): 358—372.
16. Farrera, I., Harrison, S. P., Prenlice, I. C. et al., Tropical climates at the Last Glacial Maximum: A new synthesis of terrestrial palaoclimate data, I. Vegetation, lake-levels and geochemistry, Climate Dynamics, 1999, 15: 823—856.
17. Wang, P. X., Response of Western Pacific marginal seas to glacial cycles: Paleoceanographic and sedimento-logical features, Marine Geology, 1999, 156: 5—39.
18. Harrison, S. P., Yu, G., Takahara, H. et al., Palaeovegetation: Diversity of temperate plants in East Asia, Nature, 2001, 413: 129—130.
19. Zheng, Y. Q., Qian, Y. F., Miao, M. Q. et al., Effect of Qinghai-Tibetan Snow Cover on the Summer Monsoon Climate of China, Chinese J. Atmos. Sci., 2001, 25: 137—151.
20. Liu, D. S., Zhang, X. S., Xiong, S. F. et al., Tibetan Plateau ice age environment and global cooling, Quaternary Sciences (in Chinese), 1999, 5: 385—396.
21. Clark, P. U., Alley, R. B., Pollard, D., Northern hemispere ice-sheet influences on global climate change, Science, 1999, 286: 1104—1111.
22. Webb, R. S., Rind, D. H., Lehman, S. J. et al., Influence of ocean heat transport on the climate of the Last Glacial Maximum, Nature, 1997, 385: 695—699.
23. Xue, B., Yu, G., Wang, S. M. et al., Preliminary reconstruction of spacial precipitation patterns and atmosphereic circulations in China during the late Quaternary, Chinese Science Bulletin, 2001, 46 (supp.): 22—27.
24. An, Z. S., Wang, S. M., Wu, X. H. et al., Eolian evidence from the Chinese Loess Plateau: The onset of the Late Cenozoic Great Glaciation in the Northern Hemisphere and Qinghai-Xizang Plateau uplift forcing, Science in China, Ser. D, 1999, 42(3): 258—271.
25. Yu, G., Xue, B., Wang, S. M. et al., Lake records and the LGM climate in China, Chinese Sci. Bull., 2000, 45: 250—255.
26. Jia, Y. L., Shi, Y. F., Wang, S. M. et al., Lake-expanding events in the Tibetan Plateau since 40ka B.P., Science in China, Ser. D, 2001, 44(supp.): 302—315.
27. Shi, Y. F., Zheng, B. X., Yao, T. D., The glacier and environment at Last Glacier Maximum in Tibetan Plateau, Glacier and Frozen Soil (in Chinese), 1997, 19: 97—113.
28. Yu, G., Xue, B., Liu, J. et al., Lake Records from China and the Palaeoclimate Dynamics (in Chinese), Beijing: China Meteorology Press, 2001, 84—95.
29. Liu, X. D., An, Z. S., Hao, X. H. et al., East Asian paleoclimate of the Last Glacial Maximun in an atmospheric general circulation model and from geological records, Proc. 30 th Int'l Geol. Congr.,1997, 21: 156—171.
30. Meng, X. W., Du, D. W., Liu, Z. X. et al., Molecular biomarker record of paleocenaographic environment in the East China Sea during the last 35,000 years, Science in China, Ser. D, 2002, 45(2), 184—192.
31. Kuhle, M., Topography as a fundamental element of glacial systems, Geojournal, 1988, 17: 545—568.